CMS Physics Analysis Summary

Contact: cms-pog-conveners-jetmet@cern.ch 2010/04/16

Calorimeter Jet Quality Criteria for the First CMS Collision Data

The CMS Collaboration

Abstract

While the CMS data quality monitoring effort intends to identify and address un-physical energy deposits in the calorimeters originating, e.g., from instrumental malfunctions or noise, at the level of calorimeter towers, and hence before jet reconstruction, we anticipate scenarios for which these efforts are not completely successful: unforeseen detector effects might lead to un-physical (fake) jets, especially in first collision data. We demonstrate how these jets are extracted from non-collision data samples in order to derive a set of jet quality criteria which efficiently reject fake jets. We present the methodology to derive the efficiencies for good jets to pass such a selection from collision data dijet events so that simulated efficiencies can be calibrated to data.

1 Introduction

The CMS Collaboration has devised and implemented an extensive operation to monitor the quality of the collision data recorded by the individual subdetectors. Dedicated personnel will be devoted around the clock to compare numerous aspects of the collected data by comparison to the respective reference distributions, both online while the data is being taken and offline after it has been transferred to mass storage. Unphysical energy deposits in the CMS calorimeters induced by e.g. noise, hot cells, or occasional malfunctions of the detector electronics will be treated appropriately [1]: either by masking the relevant channels such that they will not be considered for e.g. the subsequent reconstruction of calorimeter jets, or by flagging the affected events or even runs to be discarded for physics analysis.

Despite the above described data quality monitoring (DQM) effort to identify and handle calorimeter noise prior the reconstruction of jets, at any given point in time new and unanticipated problems can arise. The desired low-lewel solution of these might need time to be identified, developed, and implemented, with a significant amount of data recorded in the meantime. We therefore propose a strategy to establish the affected data sample for physics analysis based on the identification of jets arising from fake calorimeter signals and a dedicated set of jet quality criteria to reject these fakes, commonly referred to as "Jet Identification" or "Jet ID". We furthermore outline the methodology to derive the efficiency of any such selection from the collision data sample itself. We consider this high-level approach as an addition to the CMS DQM operation in order to further strengthen it.

Collider data may contain an admixture of real jets originating from the primary interaction, jets from accelerator induced backgrounds, and from un-physical, such as jets due to detector noise. In this paper we address the third category. There are several ways to record a sample consisting of pure fake jets of this type in order to characterize them and to develop selection criteria to efficiently reject them. So called "cosmic runs" yield non-collision data samples free of any physical jets, and we anticipate that CMS will routinely collect such samples during LHC quiet time. Selecting events in the LHC abort gaps yields a complimentary fake jet sample uncovering potential effects due to the concurrent operation of the LHC machine and the CMS calorimeters. In Section 6 we furthermore present strategies to select collision data samples enriched in unphysical jets, to to identify additional effects that might occur in the presence of physical energy flow from hard proton-proton collisions.

Before the LHC is scheduled to provide first collisions towards the end of 2009, the CMS detector is operated continuously in cosmic runs, yielding valuable information towards a good understanding of all its subsystems. As an illustration of the approaches outlined in this document, we study a subset of the non-collision data sample recorded during the "*Cosmic Global Run at almost Four Tesla*" (CRAFT 2008). We stress that most of the calorimeter problems underlying the jets in this sample will not be relevant in the future as their sources were identified and fixed on hardware and DQM levels. We nevertheless take this dataset as an example and demonstrate how to derive jet quality selection criteria which reject unphysical jets efficiently, while retaining the vast majority of physical jets in simulated samples.

All presented studies are based on jets reconstruction with the SISCone [2] jet clustering algorithm, with a jet size parameter of $R = 0.5$. Only calorimeter towers passing the standard CMS thresholds in energy E and transverse energy E_{T} are considered. The standard CMS jet energy corrections [3] are applied unless otherwise noted. All presented concepts are applicable just as well to other jet algorithms or tower thresholds.

Note that while the identification of jets belonging to the hard interaction of the event and the

rejection of jets arising from pile-up interactions can justifiably be labeled "Jet ID" as well, these problems are not considered here. Nevertheless, the described methodology for calibrating jet ID efficiencies will be just as suitable to address these problems.

2 The CMS Detector

A detailed description of the Compact Muon Solenoid (CMS) experiment can be found elsewhere [4]. Figure 1 shows a schematic view of CMS which includes most components relevant for the presented studies. The central feature of the CMS apparatus is a super-conducting solenoid, of 6 m internal diameter. Within the field volume are the silicon pixel and strip tracker, the crystal electromagnetic calorimeter (ECAL) and the brass-scintillator hadronic calorimeter (HCAL). The calorimeter cells are grouped in projective towers, of granularity $\Delta\eta \times \Delta\varphi = 0.087 \times 0.087$ at central rapidities and 0.175×0.175 at forward rapidities. A calorimeter tower in the barrel consists of one or two hadronic and 25 (5×5) electromagnetic calorimeter cells, and the composition in other detector regions is similar. The outer hadronic calorimeter (HO) is situated in the barrel outside the magnetic coil to ensure adequate sampling depth, but is not used in the jet clustering for these studies.

Besides the barrel (EB and HB) and endcap (EE and HE) detectors, CMS has extensive forward calorimetry (HF), which covers the range $3.0 < |\eta| < 5.0$, not shown in Figure 1. It consists of a large steel block which serves as the absorber with active quartz fibers embedded running parallel to the LHC beam-line. The energy measurement is based on the detection of the Cherenkov light in the quartz fibers which is emitted by incident particles traversing the absorber. The HF calorimeter provides twofold longitudinal segmentation as follows: half of the fibers run over the full depth of the absorber (165 cm) and are referred to as *long fibers*, while the other half starts at a depth of 22 cm from the front of the detector, referred to as *short fibers*. Long (L) and short (S) fibers are read out separately and thus allow for showers induced by electrons and photons, which deposit a large fraction of their energy in the first 22 cm, to be distinguished from those generated by hadrons, which tend to produce equal signals in both calorimeter segments on average.

We will refer to specific coherent noise patterns in Section 4 which are intimately related with the segmentation of the HB and HE detectors and the corresponding electronic readout schemes. The HB consists of 36 identical azimuthal wedges which form two half-barrels around the beamline. Each wedge is segmented into four azimuthal angle (φ) sectors, and each half-barrel is further segmented into 16 η towers. The readout chain channels the light from the active scintillator layers from one φ-segment and all η-towers of a half-barrel to a hybrid photo-diode (HPD). The HPDs associated with the four φ-segments of a single wedge are grouped together into one readout box (RBX). Thus, the occurrence of electronic noise across all channels of either an HPD or even an entire RBX will lead to the corresponding and very distinct patterns in $\eta \times \varphi$. CMS intends to detect these patterns prior to jet reconstruction and either remove such deposits or reject the respective events. The confirmation of a known problem of this kind using jets nevertheless demonstrates the usefulness of jets to identify similar problems in the future.

We consider five different $|\eta|$ regions which are based on the geometry of the CMS calorimeters in general and the HCAL in particular, taking into account that a jet extends in η (and φ) beyond its axis:

- **HB**: $|\eta| < 1.0$ (barrel region)
- **BE**: $1.0 < |\eta| < 1.75$ (transition region between barrel and endcap)

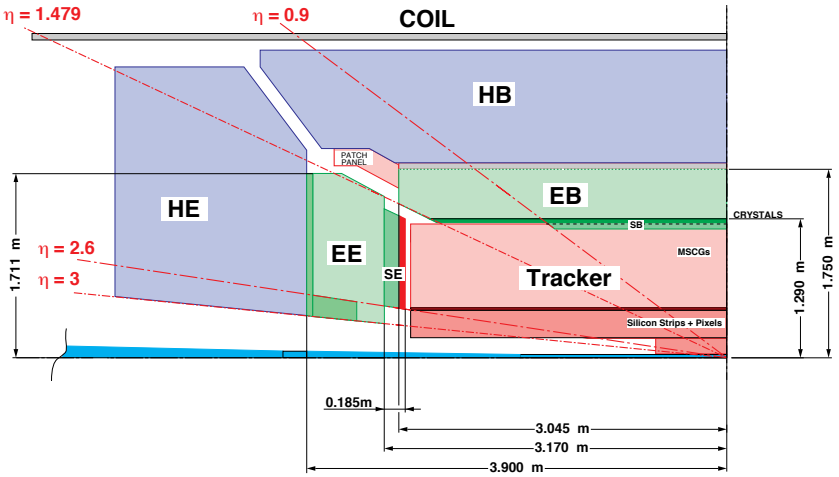

Figure 1: Schematic view of one quadrant of the CMS calorimetry and tracking system. The forward calorimeter HF covering $3.0 < |\eta| < 5.0$ is not shown.

- **HE**: $1.75 < |\eta| < 2.55$ (endcap region)
- **EF**: $2.55 < |\eta| < 3.25$ (transition region between endcap and forward)
- **HB**: $|\eta| > 3.25$ (forward region)

3 Jet ID variables

A set of jet variables to be considered in order to asses the likelihood of a jet originating from the interaction of the colliding proton beams and not detector malfunction or electronic noise is listed below. Most of the quantities are based on the confirmation of the presence of the jet by more than one subdetector, for example: central tracks pointing in the direction of a jet make up a sizeable fraction of the jet energy as measured in the calorimeters; the jet energy is distributed among the electromagnetic and hadronic calorimeter cells; or a forward jet induced a signal in both the long and short fibers, which are readout separately. This strategy and therefore the associated variables are not specific to any particular collider experiment. We use several such variables in this paper:

- f_{EM}: fraction of jet energy contributed by ECAL energy deposits.
- N_{towers}: the total number of calorimeter towers clustered into a jet.
- N^{90}_{towers}: the minimum number of calorimeter towers clustered into a jet which contain 90 % of the jet energy.
- N^{90}_{cells}: the minimum number of ECAL and HCAL cells clustered into a jet which contain 90 % of the jet energy.
- $\sigma_{\varphi\varphi}$: the RMS of the E_{T}-weighted φ distribution of the calorimeter towered clustered into a jet.

This concept could be further exploited in the transition regions, e.g. by requiring energy depositions in both HB and HE for a jet with $\eta = 1.5$. Such strategies require further studies but could help understand the jet rates for the challenging overlap regions.

Some of the variables are instead based on the shape of the cluster of jet energy depositions in a single subsystem, which is expected to be somewhat circular in $\eta \times \varphi$ for physical jets, while coherent noise spread over a number of readout channels often leads to distinct patterns

corresponding to the readout segmentation. The corresponding quantities R_{HF}, f_{HPD}, and f_{RBX} listed below are specific to the CMS detector and the particular design of its data acquisition:

- $\boldsymbol{R_{\mathrm{HF}}}$: $(E_{\mathrm{S}} - E_{\mathrm{L}})/(E_{\mathrm{S}} + E_{\mathrm{L}})$, where E_{S} and E_{L} are the energies measured in the short and long fibers of the HF calorimeters respectively, see Section 2.
- $\boldsymbol{f_{\mathrm{HPD}}}$: fraction of energy contributed by the hottest (highest energy) HPD readout
- $\boldsymbol{f_{\mathrm{RBX}}}$: fraction of energy contributed by the hottest RBX

4 Fake Jets in Cosmic Global Runs

In this section we illustrate the principles of a jet ID study using non-collision events containing only fake jets to assess the necessity of jet quality criteria, and to derive them. We analyze a subset of the events recorded during the CRAFT 2008 cosmic run. This run represented an important commissioning milestone of the CMS detector, as it was operated at the nominal magnetic field of 3.8 T and recorded detector signals from almost all subsystems, induced primarily by cosmic muons. In the absence of LHC collisions, the collected dataset is free of any physical jets and thus provides a large sample of fake jets, the properties of which are studied. While the principles to draw conclusions about the nature and source of fake jets based on non-collision date described in the following are quite generic, and applicable to future datasets with potentially different problematic features, we emphasize again that the presented results are based on detector problems which were since understood and addressed, thanks to the valuable insights provided by this data sample.

The methodolgy described in the following is however applicable to future datasets with potentially different problematic features than the one studied here as an example.

We select events without requiring particular triggers and without applying any data quality criteria, requiring the leading jet in the event to exceed $p_{\mathrm{T}} > 20\,\mathrm{GeV}$. We subdivide the selected events into the *HBHE* (10k events) and *HF* (1.3 million events) samples, considering only jets which fulfill $|\eta| < 3.0$ and $|\eta| > 3.0$ respectively. A few calorimeter regions with abnormally high occupancies were identified, and jets from these regions are discarded in all three samples.

The N_{towers}, p_{T}, and f_{EM} distributions for jets in the HBHE non-collision data sample are shown in Figure 2. The jets reconstructed in CRAFT data are dominated by low p_{T} jets consisting mostly of few calorimeter cells with energy deposits just above the applied reconstruction threshold. The f_{EM} distribution indicates that the overwhelming majority of these *soft fakes* can be identified by their lack of energy in the electromagnetic calorimeters: f_{EM} is below 0.001 for $\approx 96\,\%$ of these jets. Physical jets with $f_{\mathrm{EM}} = 0$ only occur for $p_{\mathrm{T}} < 50\,\mathrm{GeV}$ at the per cent level, as illustrated later in Figure 6.

In order to understand origin and properties of *hard fakes* we first look at jets with significant electromagnetic energy fraction. The N_{towers} and η-φ distributions for jets with $f_{\mathrm{EM}} > 0.5$ are shown in Figure 3. Jets containing less than 20 calorimeter towers (red histogram entries) are likely to originate from muons, while a subset of those with $N_{\mathrm{towers}} > 20$ (green histogram entries) are localized around $\eta = 1$ and $\varphi = -2$. This location confirms a known ECAL noise pattern detected by the data quality monitoring and shown to be present only for a short data taking period. The respective runs were flagged as bad and discarded from further analysis.

We then identify several sources of hadronic noise from the peak structure of the N_{towers} distribution of the HBHE sample in Figure 2. Each peak indicates the presence of distinct effects: $N_{\mathrm{towers}} \approx 10$ corresponds to HPD noise in the HB, where the fake signals from all 16 channels

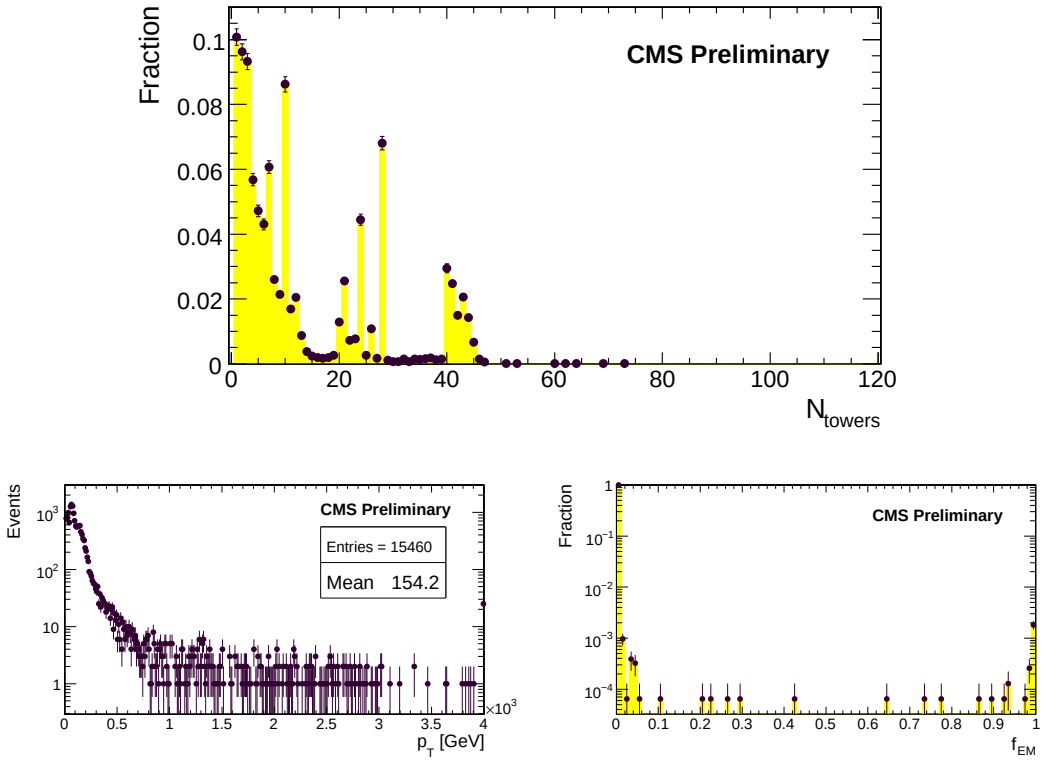

Figure 2: Calorimeter jet N_{towers}, p_{T}, and f_{EM} distributions for the HBHE non-collision data sample.

due to electric discharge lead to the reconstruction of two jets; $N_{\text{towers}} \approx 24$ and $N_{\text{towers}} \approx 40$ correspond to RBX noise in the HB, where the fake signals from all 64 channels due to data corruption lead to the reconstruction of two jets with these number of calorimeter towers respectively. Similar arguments regarding the choice of the jet cone of $R = 0.5$ and the geometry of the cells associated with a single HPD or RBX link the other peaks with the corresponding effects in the HE. Figure 4 (left) illustrates the properties of fake jets in the HE originating from RBX noise, by selecting jets with $20 \leq N_{\text{towers}} < 30$ and low electromagnetic fraction $f_{\text{EM}} < 0.08$. These jets are characterized by $f_{\text{RBX}} \approx 1$. The jets displayed on the right of Figure 4 are selected by requiring $N_{\text{towers}} = 10$ and additionally $\sigma_{\varphi\varphi} < 0.004$, yielding a jet sample dominated by fakes originating from HPD noise in the HB, with f_{HPD} close to one.

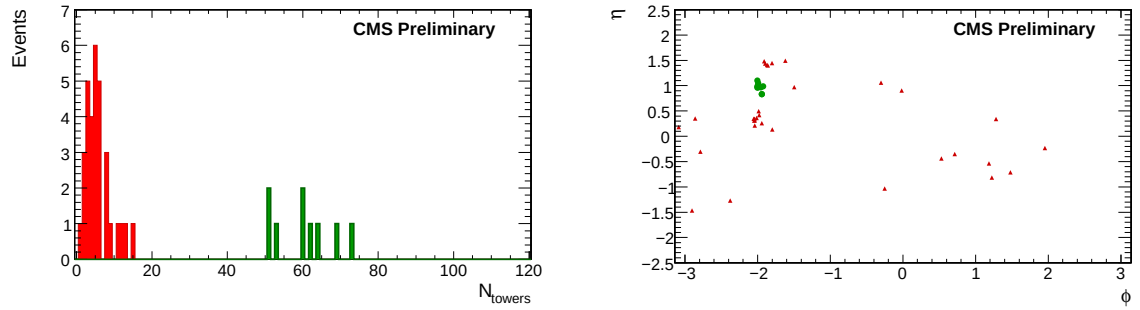

Figure 3: N_{towers} (*left*) and η-φ distributions for jets in the HBHE sample with $f_{\text{EM}} > 0.5$. The green entries (full circles) in the plots on right correspond to the excess observed at $\eta = 1$ and $\varphi = -2$.

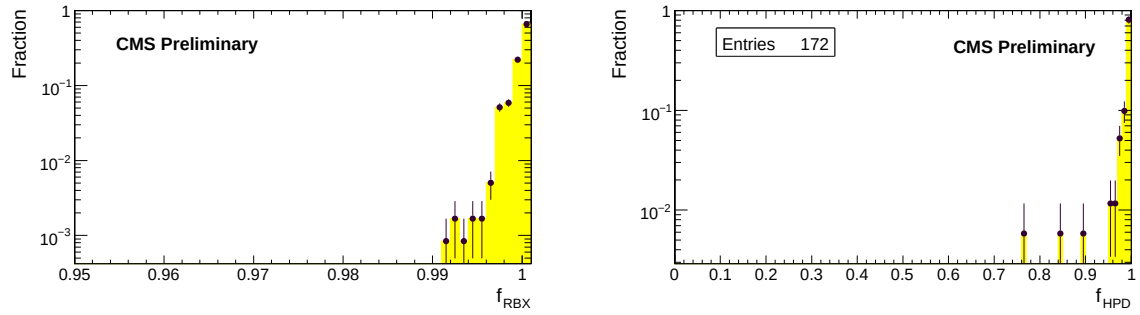

Figure 4: *Left*: f_{RBX} distribution for jets in the HBHE sample with low electromagnetic fraction $f_{\text{EM}} < 0.08$, $20 \leq N_{\text{towers}} < 30$, $1.3 < |\eta| < 3.0$, and $40 < p_{\text{T}} < 500\,\text{GeV}$. The N_{towers} selection zooms in on jets originating from RBX noise as explained in the text. *Right*: f_{HPD} distribution for jets in the HBHE sample with $N_{\text{towers}} = 10$ and $\sigma_{\varphi\varphi} < 0.004$, selecting jets originating from HPD noise in the HB as outlined in the text.

To identify and reject unphysical jets in the HF (*forward fakes*), we study the R_{HF} variable defined in Section 3: jets originating from pp interactions are expected to deposit energy in both the short and long fibers of the HF, which are readout separately, and $|R_{\text{HF}}| = 1$ indicates signals in only one of the two, as confirmed in the corresponding distribution shown in Figure 5. This can happen when energetic particles hit the photo-multipliers, either due to the direction of the incoming cosmic muons in non-collision data, or due to the tail end of hadronic showers in collision data.

Based on these studies, we define two sets of standard jet quality selection criteria, "**loose**" and "**tight**", which are found to efficiently reject the unphysical jets in the CRAFT 2008 sample. The

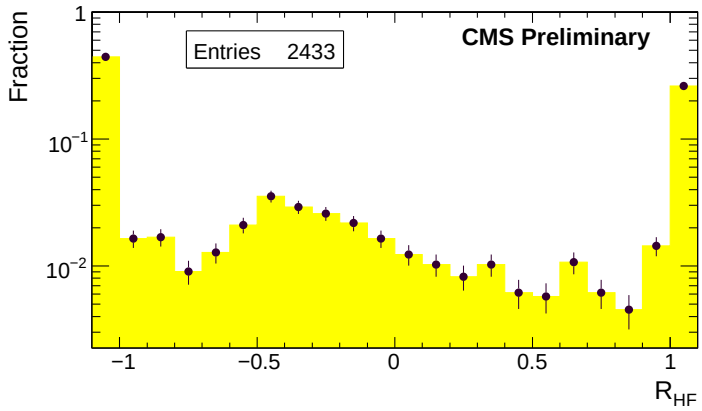

Figure 5: R_{HF} distribution of jets in the HF sample. $|R_{\mathrm{HF}}| = 1$ strongly indicates unphysical jets as explained in the text.

criteria below are as much for illustration as the analysis of the data, and they will be refined soon with data taken during the upcoming CRAFT 2009 cosmic run, where we expect the CMS detector to be operated with a setup very similar to the startup of the LHC. Note that the selection cuts are chosen as well to be minimally biasing and highly efficient, and in Section 5 it will be described in some detail how these efficiencies can be determined from the collision data itself.

The loose calorimetry based selection cuts are:

- $f_{\mathrm{HPD}} < 0.98$
- $N^{90}_{\mathrm{cells}} \geq 2$
- $f_{\mathrm{EM}} > 0.01$, for jets in HB, BE, and HE
- $R_{\mathrm{HF}} > -0.9$, for jets in HF
- $R_{\mathrm{HF}} < 1$, for jets in HF with $p_{\mathrm{T}} > 80\,\mathrm{GeV}$.

The tight calorimetry based selection cuts are (on top of the above loose criteria):

- $f_{\mathrm{HPD}} < 0.95$, for jets with $p_{\mathrm{T}}^{\mathrm{raw}} > 25\,\mathrm{GeV}$
- $f_{\mathrm{EM}} < 1$, for jets in BE and HE with $p_{\mathrm{T}} > 80\,\mathrm{GeV}$
- $-0.3 < R_{\mathrm{HF}} < 0.9$, for jets in HF with $p_{\mathrm{T}} < 50\,\mathrm{GeV}$
- $-0.2 < R_{\mathrm{HF}} < 0.8$, for jets in HF with $50 < p_{\mathrm{T}} < 130\,\mathrm{GeV}$
- $-0.1 < R_{\mathrm{HF}} < 0.7$, for jets in HF with $p_{\mathrm{T}} > 130\,\mathrm{GeV}$,

where $p_{\mathrm{T}}^{\mathrm{raw}}$ is the uncorrected calorimeter jet transverse momentum. The f_{EM}, N^{90}_{cells}, f_{HPD}, and R_{HF} distributions for tag & probe selected jets in a QCD dijet MC sample (see Section 5) are shown in Figure 6 for three different jet p_{T} ranges. Note that the R_{HF} windows in particular trace the edges of the distribution predicted for jets originating from the primary interaction according to the simulation.

Based on simulation studies we anticipate that the addition of tracking information will be powerful to reject noise, but stringent requirements quickly lead to significant inefficiencies for real jets, which therefore will have to be quantified properly. We therefore plan to use a moderate requirement which appears to remove insignificant amounts of real jets: the presence of a single well-measured charged particle track with $p_{\mathrm{T}} > 1\,\mathrm{GeV}$ matched to the jet within

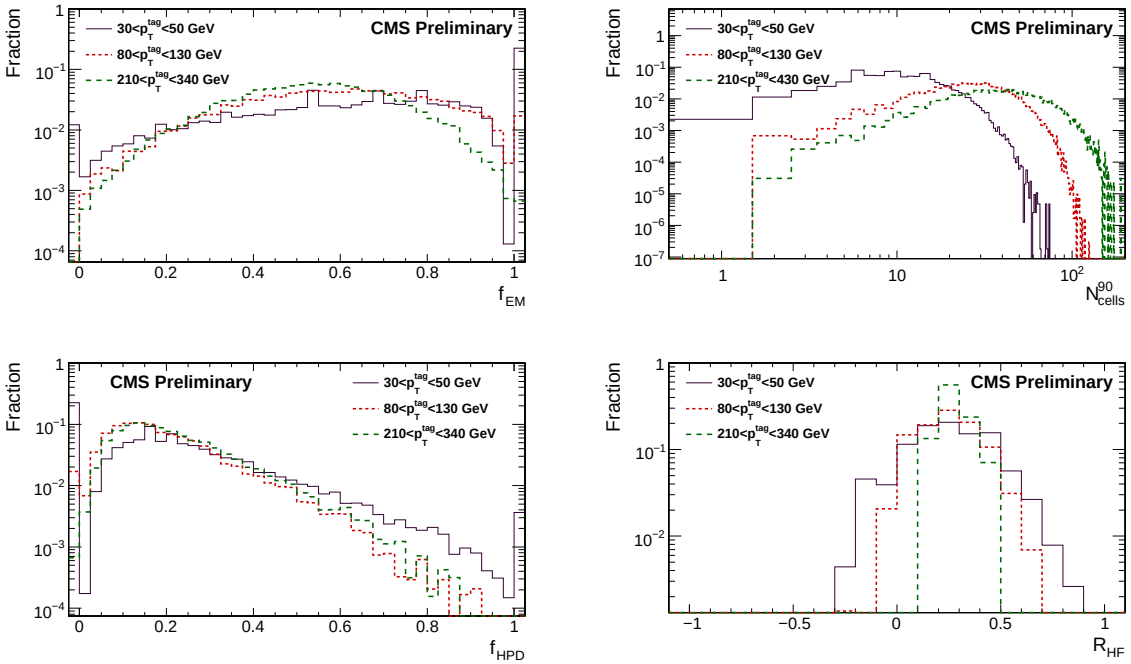

Figure 6: f_{EM}, N^{90}_{cells}, and f_{HPD} distributions for jets in the HB, and R_{HF} distribution for jets in the HF region, for jets in a QCD dijet MC sample.

$\Delta R < 0.5$.

5 Data-driven determination of quality cut efficiencies

Experience from past collider experiments as well as from the ongoing CMS commissioning efforts suggest that the effects which make jet quality criteria necessary in the first place are typically intimately related to atypical behavior and the subtleties of the hardware and electronics of the involved subsystems, and therefore not properly modeled by the simulation. We therefore propose a data-driven procedure to measure the (in-) efficiency of any set of jet selection criteria, which was successfully employed by the Tevatron experiments and does not rely on Monte Carlo truth information. The technique can therefore be applied to both collision data and simulation samples in order to calibrate the Monte Carlo. Here, we apply this methodology to simulated QCD dijet events in order to extract a sample which contains almost no fake jets, and compute inefficiencies which are then trusted to indicate if a particular cut as suggested in Section 4 will remove only a negligible amount of jets arising from the hard interaction.

To select a dijet sample which is unbiased and practically free of unphysical jets, a tag & probe approach is applied (illustrated in Figure 7): events are selected based on single jet triggers with various p_{T} thresholds for which the two leading jets are back-to-back in azimuth and there is little additional activity. The tag jet must match the jet which fired the trigger, and have at least one confirming good track measured by the CMS pixel and silicon detectors associated through matching in η-φ space. The unbiased probe jet is then used to determine the (in-) efficiency of any selection criteria.

To select cuts which are back-to-back, we apply a cut on the azimuthal angle between the two leading jets, $\Delta\varphi$, more conveniently expressed as the complementary angle $\delta = \pi - \Delta\varphi$. Ad-

ditional activity is vetoed by imposing an upper limit on the transverse momentum $p_{\mathrm{T}}^{\mathrm{3rd}}$ of the third jet in the event. The differential cross-section as a function of jet p_{T} and the δ distributions for various p_{T} ranges of the tag jet are shown in Figure 8.

The resulting unbiased sample of probe jets contains practically no unphysical jets and can be used to extract the efficiency of any quality selection, defined as the number of probe jets passing the selection criteria divided by the total number of probe jets. We choose to consider the inefficiency instead, which is equivalent but captures the cost of any such requirements, namely the rejection rate of real jets originating from the hard interaction. Inefficiency are determined as a function of jet p_{T}. To avoid biases due to the steeply falling nature of the QCD dijet p_{T} spectrum in association with the jet energy resolution, coupled with the correlation of the jet energy response and most of the relevant variables sensitive to jet quality, the inefficiency is determined in bins of $p_{\mathrm{T}}^{\mathrm{tag}}$, where the inefficiency measured in each individual bin is associated with its average $< p_{\mathrm{T}}^{\mathrm{tag}} >$. The inefficiencies are then remapped to the probe p_{T} by associating the average probe $< p_{\mathrm{T}} >$ in each $p_{\mathrm{T}}^{\mathrm{tag}}$ bin to its average $< p_{\mathrm{T}}^{\mathrm{tag}} >$.

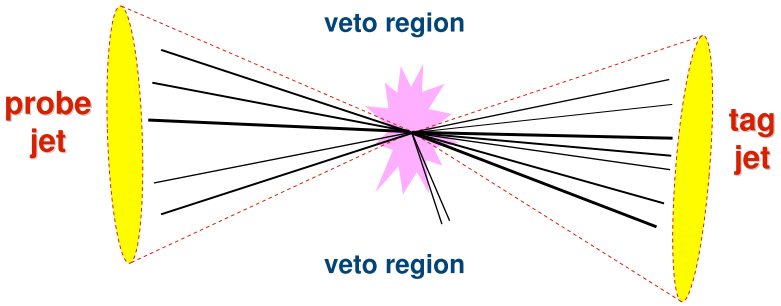

Figure 7: Sketch of the tag & probe event selection to extract an unbiased sample of (probe-) jets originating from the hard interaction.

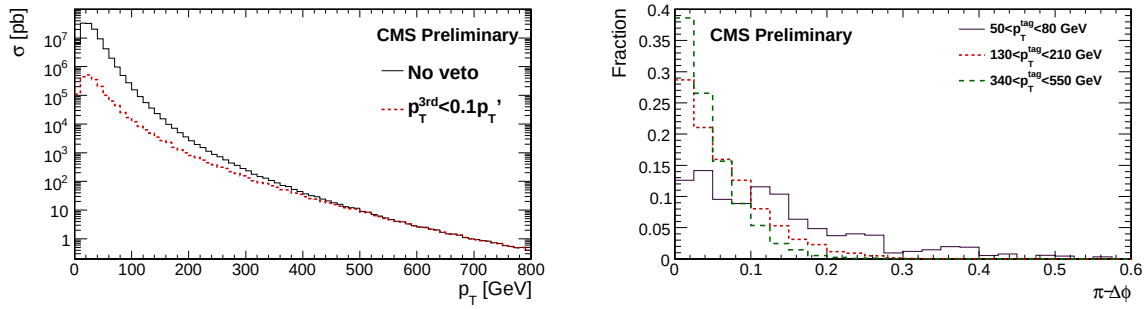

Figure 8: *Left*: differential jet cross-section as a function of jet p_{T} with (*dashed red histogram*) and without (*black solid histogram*) the tight veto against additional activity in the dijet event. $p_{\mathrm{T}}^{\mathrm{tag}}$ refers to the tag jet p_{T}. *Right*: $\delta = \pi - \Delta\varphi$ between the two leading jets in the event, for different p_{T} ranges of the tag jet.

6 Selection of Fake-Jets from Collision Data

We so far described how to extract a sample of pure fake jets from non-collision data. However, collision data might contain un-physical jets which are not represented by non-collision data. To discover, study, and ultimately reject such jets, we suggest possible strategies to collect samples of collision events enriched in fake jets. We propose three different selections which will

yield different such samples, each with different associated biases such that they might reveal different sources of noise:

Track-Veto: a jet sample can be enriched in fake jets by requiring one or more jets not to be associated with any good track measured by the CMS pixel and silicon detectors. The selection can be refined by basing the veto on e.g. the fraction of jet energy as measured by the calorimeters to be confirmed by the energy of all tracks spatially associated with the jet to be significantly below the average expectation.

Too-Many-Jets: events with high jet multiplicity are naturally enriched in un-physical jets. The selection can be combined with the Track-Veto described above.

Third-Jet: selecting events with two well-balanced jets which pass the standard quality selection criteria, with an additional jet which is not confirmed by any tracks and therefore likely to be a fake jet.

The optimization of any such selection can be be attempted using simulation samples with noise from non-collision data overlaid, but should ultimately be refined and validated with collision data.

7 Conclusions

We proposed strategies to extract and analyze pure fake jet samples from non-collision data and illustrated the derivation of a set of quality criteria which efficiently reject unphysical jets accordingly. A data-driven tag & probe approach to measure the (in-)efficiency for physical jets originating from the hard interaction based on QCD dijet events was presented as well. We briefly outlined possible strategies to select collision data samples enhanced in fake jets in order to study unphysical jet properties in the presence of physical energy flow from hard proton-proton collisions.

We analyzed a non-collision data sample recorded during the CRAFT 2008 cosmic run, where a number of calorimeter problems suitable to illustrate the concepts of this approach were found. However, these problems were identified and understood by the CMS data quality monitoring efforts without the use of clustered jets, and all of them were properly addressed and are therefore irrelevant by now. Nevertheless, we anticipate that the described strategies and methods, which were already successfully employed e.g. at the Tevatron experiments, will be suitable to address similar detector effects relevant to the quality of calorimeter jets in the future. It is important for CMS to establish this second line of defense in order to enable sound and timely physics analysis in case un-physical jets find their way past the data quality certification into the data sample at a non-negligible rate.

8 Acknowledgements

We thank the technical and administrative staff at CERN and other CMS Institutes, and acknowledge support from: FMSR (Austria); FNRS and FWO (Belgium); CNPq, CAPES, FAPERJ and FAPESP (Brazil); MES (Bulgaria); CERN; CAS, MST and NSFC (China); MST (Croatia); RPF (Cyprus); Academy of Sciences and NICPB (Estonia); Academy of Finland, ME and HIP (Finland); CEA and CNRS/IN2P3 (France); BMBF, DFG and HGF (Germany); GSRT and Leventis Foundation (Greece); OTKA and NKTH (Hungary); DAE and DST (India); IPM (Iran); SFI (Ireland); INFN (Italy); KICOS (Korea); CINVESTAV, CONACYT, SEP and UASLP-FAI (Mexico); PAEC (Pakistan); SCSR (Poland); FCT (Portugal); JINR (Armenia, Belarus, Georgia, Ukraine,

Uzbekistan); MST and MAE (Russia); MSD (Serbia); MCINN and CPAN (Spain); Swiss Funding Agencies (Switzerland); NSC (Taipei); TUBITAK and TAEK (Turkey); STFC (United Kingdom); DOE and NSF (USA).

References

[1] **CMS** Collaboration, "Anomalous signals in ECAL and HCAL", *CMS PAS* **CFT-09-019** (2009).

[2] G. P. Salam and G. Soyez, "A practical seedless infrared-safe cone jet algorithm", *JHEP* **0507:086** (2007).

[3] **CMS** Collaboration, "Plans for Jet Energy Corrections at CMS", *CMS PAS* **JME-07-002** (2008).

[4] **CMS** Collaboration, "The CMS Experiment at the CERN LHC", *JINST* **3** (2009) S08004.